Application of the COMPASS-FP Beta Version to the Reactor Vessel in the APR1400 for Predicting Aerosol Behavior under a Severe Accident

Hyung Seok Kang[*], Bo Wook Rhee, Dong Ha Kim

Korea Atomic Energy Research Institute, 989-111, Daedeok-daero, Yuseong, Daejeon, 305-353, Republic of Korea
[*]Corresponding author: hskang3@kaeri.re.kr

1. Introduction

We developed the COMPASS-FP beta version for predicting radioactive aerosol behavior in the RCS in a nuclear power plant [1,2]. However, it is necessary to see that the developed COMPASS-FP beta version can produce reasonable results in a real plant using CSPACE results [3] obtained from a simulation for the severe accident because only the gravitational settling model in the COMPASS-FP was compared with the test data of ABCOVE-5, 6, and 7. We may know that the predicted aerosol behavior results are reasonable by estimating the variation of the aerosol removal rates according to various model parameters used in the aerosol removal models.

2. Development of the COMPASS-FP Beta Version

The purpose of the COMPASS-FP beta version is to calculate the transport of the radioactive aerosol mass by integrating the overall size distribution of the aerosol particles in the RCS during a severe accident. A governing equation for the rate of mass change of the group-i aerosol in a control volume ($dm_{Ai/dt}$) can be defined as Eq. (1). To calculate each term in the right-hand side of Eq. (1), aerosol transport and generation, the fission product release model with an empirical correlation, the aerosol generation model [3], and the aerosol transport model were implemented in the COMPASS-FP beta version [1,2]. The aerosol usually flows with the steam and hydrogen streams along the RCS loop during or after the aerosol generation process. The aerosol in the mixture flow may be deposited on the RCS wall by various mechanisms such as gravitational settling (λ_{sed}), inertia deposition (λ_{imp}), diffusiophoresis (λ_{diff}), and thermophoresis (λ_{th}). The total removal rate (λ_t) in Eq. (1) is the summation of four mechanisms as Eq. (2).

$$\frac{dm_{Ai}}{dt} = W_{Ai,\,in} - W_{Ai,\,out} - \lambda_t m_{Ai} + G_i \qquad (1)$$

$$\lambda_t = \lambda_{sed} + \lambda_{imp} + \lambda_{diff} + \lambda_{th} \qquad (2)$$

3. CSPACE Calculation Results for a Sever Accident

The CSPACE analysis was conducted for the severe accident including the core degradation phenomenon initiated by LBLOCA (Large Break Loss Of Coolant Accident) occurred at the cold leg in the LOOP-B of the APR1400. In the CSPACE analysis, the thermal-hydraulic calculation was performed by the SPACE 2.16 and the core degradation in the reactor vessel by the COMPASS 2.2 [4]. Fig. 1 shows the CSPACE nodalization model for simulating the severe accident analysis of the APR1400 [3]. The reactor vessel is composed of a downcomer, a lower plenum, a lower head, an upper plenum, an upper head, and a core. The reactor core was modeled by a 3 x 5 radial channel ring configuration. The CSPACE calculation was conducted as a transient state for 4500 s with various time steps of 1.0^{-15} to 1.0^{-2} s with using the steady state results as the initial condition [3]. Fig. 2(a) shows the calculated gas temperature at the fourth node in the center ring of the core by the CSPACE. This is the highest temperature in the core nodes and it is approximately equal to the fuel cladding temperature. Figs. 2(b) and (c) are the gas temperature and the volume averaged gas velocity in the upper plenum, respectively.
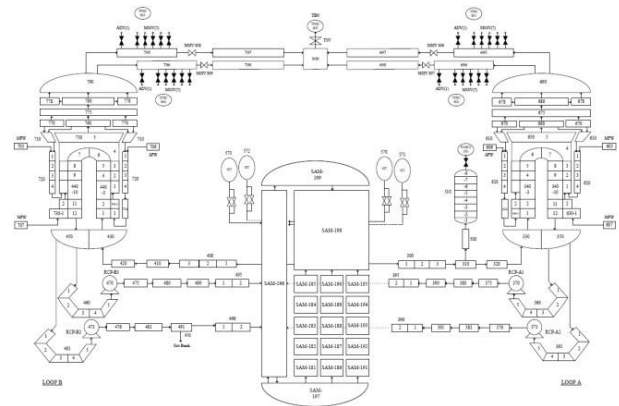
Fig. 1 Nodalization for the CSPACE Analysis [3]
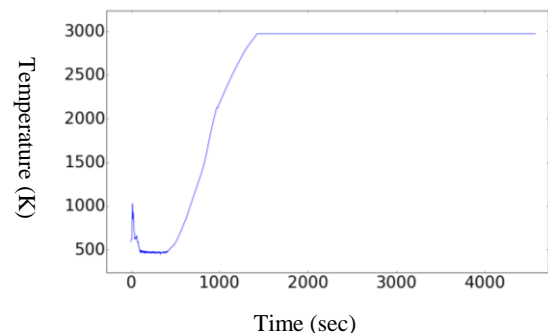
(a) Gas Temperature in the 4th node of Center Ring

(b) Gas Temperature in the upper plenum

(c) Gas Velocity in the upper plenum
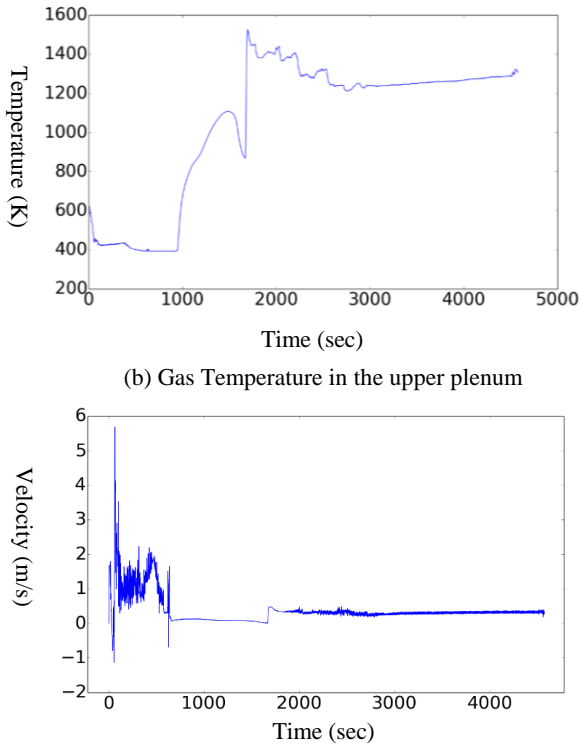
Fig. 2 CSPACE Results for a Severe Accident

4. COMPASS-FP Results using the CSPACE Data

4.1 Test Condition and Facility

The FP release model was applied to the reactor core for calculating the amount of the FP gas release using the CSPACE data, the core temperature, obtained from the simulation of the severe accident in the APR1400. The initial FP mass data was assumed as the data of the peach bottom reactor calculated by the ORIGEN2 code [5]. The predicted FP mass variation in the core and FP vapor flowing to the upper plenum are shown in Fig. 3. The calculated FP mass in Fig. 3(a) are plotted from approximately 750 s after the start of the CSPACE calculation. This is arisen that the empirical correlations of the CORSOR model can be applied when the core temperature is higher than 1173 K [6]. According to the release results of Xe, Kr, Cs, and I, the flow of Group-1 to Group-3 to the upper plenum are completed from 800 s to 1500 s after the start of the FP release model. The flow of Group-4 to Group-8 to the upper plenum are maximum at approximately 1400 s and then the FP flows of those group are gradually decreased to 4500 s. These flow patterns are resulted from the behavior of the core temperature as shown in Fig. 3(a). The calculated aerosol generation rates of Group-2 to Group-8 in the upper plenum are shown in Fig. 4. The FP vapors arrived at the upper plenum are instantly condensed to the aerosol droplet because the temperature in the

upper is lower than the boiling temperatures of Group-2 to Group-8 [2,7].
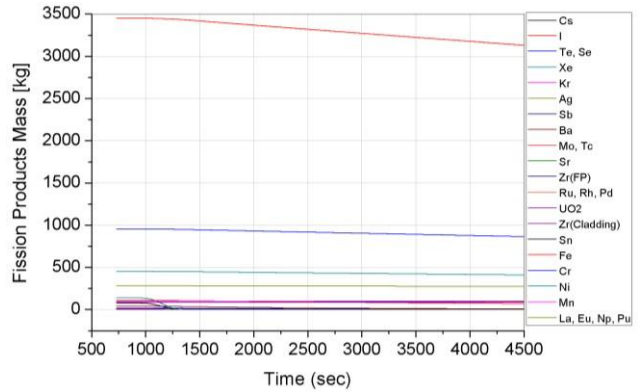
(a) FP Mass Variation in the Reactor Core
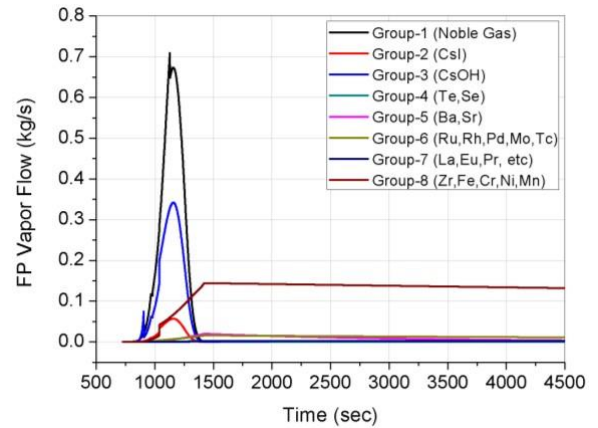
(b) FP Vapors Flowing to the Upper Plenum form Core

Fig. 3 Prediction Results by the FP Release Model
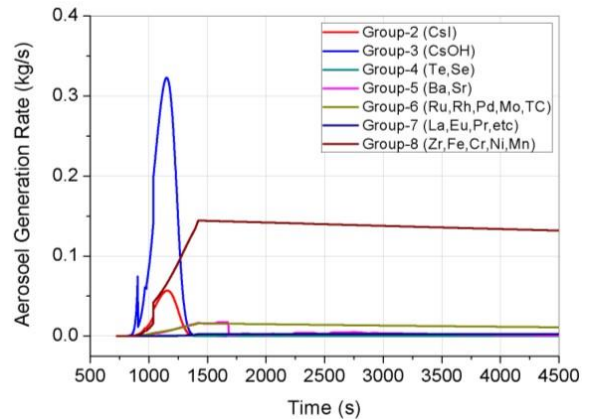
Fig. 4 Prediction Results by the Aerosol Generation Model

4.2 COMPASS-FP Calculation Results

The sensitivity calculation results of the aerosol removal models using the CSPACE data in the reactor upper plenum of the APR1400 are shown in Fig. 5. The behavior of the aerosol removal rates as time passes are resulted from the variations of the thermal-hydraulic data (temperature, density, and viscosity) and the suspended aerosol mass (m_p) in the upper

plenum (Fig. 2). The variations of the aerosol removal rates by the sedimentation for various settling areas (Eq. (3)) show that the calculated removal rates are increased as the settling area enlarges (Fig. 5(a)). These results are reasonable because the sedimentation process is proportional to the settling area size (Eqs. (4) and (5)) [1,2].

$$h_{eff} = volume / settling\ area \qquad (3)$$

$$M_{sed} = \left(\frac{\gamma^9 g h_{eff}^4 \varepsilon_o^5}{\alpha^3 K_o \mu \rho^3} \right)^{1/4} \cdot m_p \qquad (4)$$

$$\Lambda_{sed} = \left(\frac{\gamma \varepsilon_o \chi^2 \mu h_{eff}^2}{\alpha K_o g \rho} \right)^{1/2} \cdot \lambda_{sed} \qquad (5)$$

Fig. 5(b) shows that the aerosol removal rates by the inertia impaction are dependent on the gas velocity and the suspended aerosol mass in the upper plenum (Eqs. (6) and (7)). Fig. 5(c) shows the variations of the aerosol removal rates by the diffusiophoresis are affected by the different diffusion coefficient (Eqs. (8) to (10)) accounting for the FP vapors into the environment gas mixture in the upper plenum. The variation of the aerosol removal rates by the thermophoresis for various gas temperatures (T_∞) shows that the calculated removal rates are determined by the ratio of the wall temperature and the gas temperature, which are defined as (Eqs. (11) and (12)).

$$M_{IMP} = \left(\frac{\gamma K_o h_{eff}}{\chi K_o u_g} \right) \left(\frac{\chi \mu D}{\alpha^{1/3} \rho u_g} \right)^{2/5} \left(\frac{\gamma g \rho \varepsilon_o}{\alpha^{1/3} \mu K_o} \right)^{13/12} \cdot m_p \qquad (6)$$

$$\Lambda_{IMP} = \frac{h_{eff}}{u_g} \left(\frac{\chi \mu D}{\rho u_g} \right)^{2/3} \left(\frac{\gamma g \rho \varepsilon_o}{\alpha \mu K_o} \right)^{1/3} \cdot \lambda_{imp} \qquad (7)$$

$$u_{diff} = \frac{F \beta_{12}}{\tilde{\rho}_1} \ln \left[\frac{P_v - P_1(0)}{P_v - P_1(\delta)} \right] \qquad (8)$$

$$\beta_{12} = \frac{D_{12} \tilde{\rho}_1}{\delta} \qquad (9)$$

$$\lambda_{diff} = \frac{u_{diff}}{h_{eff}} \qquad (10)$$

$$u_{th} = \frac{\mu \kappa}{\chi \rho_g L} \left[\frac{T_\infty}{T_w} - 1 \right] \left[\frac{1 - (\kappa Pr)^{1.25} \left(T_w / T_\infty \right)}{1 - (\kappa Pr)^{1.25}} \right] Nu \qquad (11)$$

$$\lambda_{th} = \frac{u_{th}}{h_{eff}} \qquad (12)$$
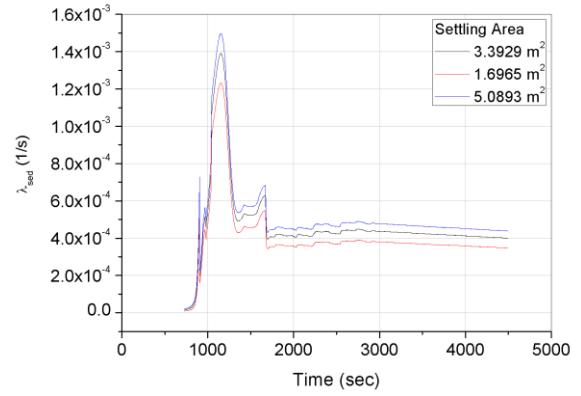
(a) Gravitational Settling
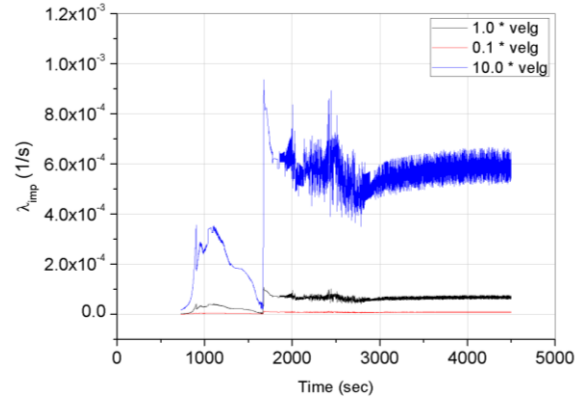
(b) Inertial Impaction
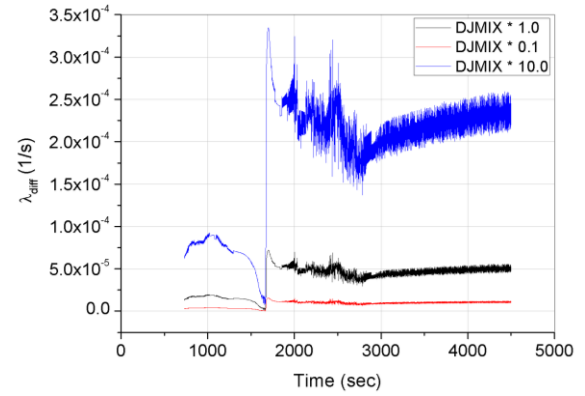
(c) Diffusiophoresis
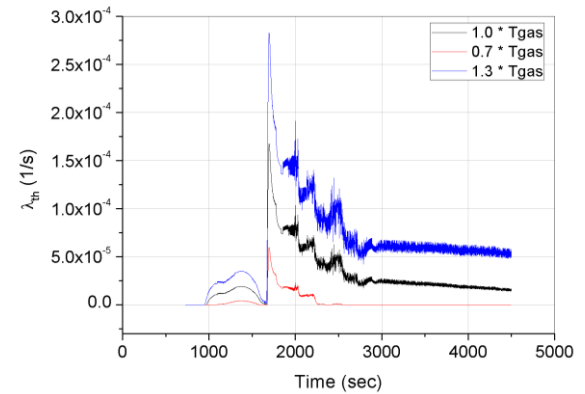
(d) Thermophoresis

Fig. 5 Prediction Results by the Aerosol Transport Model

5. Conclusions and Further Work

We applied the COMPASS-FP beta version to the reactor vessel of the APR1400 for predicting the FP gas release rate, aerosol generation rate, and aerosol removal rates. The thermal-hydraulic data by the CSPACE in the reactor vessel was used for this calculation. In addition, we performed sensitivity calculations by varying model parameters in four aerosol removal models in the upper plenum of the reactor vessel for seeing the variation of the aerosol removal rates. From the sensitivity calculation results, we found that the COMPASS beta version produced the reasonable results of the FP release rate, the aerosol generation rate, and the aerosol removal rates according to the thermal-hydraulic data in the reactor vessel of the APR1400. The beta version is being tested and the version 1.0 will be released soon with more general features for the FP release, transport and removal behaviors in the RCS.

Nomenclature

D	diffusion coefficient
G	aerosol source
h	height
K	FP gas fractional release coefficient
K_o	normalized Brownian collision coefficient
M	dimensional density of particle cloud
m	mass
m_p	mass rate of production of particles per unit volume particle cloud
P	pressure
T	temperature
u	velocity
W	mass flow rate of aerosol

Greek Letters

α	density correction factor
β	mass transfer parameter
$ε_o$	adjustable particle capture efficiency constant
χ	dynamic shape factor
γ	collision shape factor
λ	aerosol removal rate constant
Λ	dimensionless aerosol removal rate
ρ	density of particle material
μ	gas viscosity

Subscripts

A	aerosol
diff	diffusiophoresis
eff	effective
f	fission product
i	i-group
imp	impaction
l	liquid
sed	sedimentation
th	thermophoresis

REFERENCES

[1] H. S. Kang, B. W. Rhee, and D. H. Kim, "Aerosol Deposition Models in the COMPASS-FP Beta Version," The Korea Nuclear Society Spring Meeting, Jeju, Korea, May 12-13 (2016).
[2] H. S. Kang, B. W. Rhee, and D. H. Kim, "Development of a Fission Product Transport Module Predicting the Behavior of Radiological Materials during Severe Accidents in a Nuclear Power Plant," *J. of Radiation Protection and Research*, 41, No 3 (2016) (to be published in September).
[3] T. B. Lee, D. K. Lee, H. S. Lee, G. W. Lee, T. S. Choi, R. J. Park, D. H. Kim, "Preliminary Evaluation of CSPACE for a Station Blackout Transient in APR1400," The Korea Nuclear Society Spring Meeting, Jeju, Korea, May 12-13 (2016).
[4] D. H. Kim, etc., Annual Report of Development of Severe Accident Code and Methodology, Technical Report, KAERI (2016).
[5] C. S. Cho, Modeling and analysis of radionuclide transport during severe accidents in boiling water nuclear reactors, Ph.D thesis, RPI, US, (1992).
[6] USNRC, "CORSOR user's manual," NUREG/CR-4173, (1985).
[7] I. Barin and O. Knacke, Thermochemical Properties of Inorganic Susbstances, Berlin, Springer-Verlag (1973).